Journal of Natural Gas Science and Engineering 47 (2017) 114–123

Contents lists available at ScienceDirect

Journal of Natural Gas Science and Engineering

journal homepage: www.elsevier.com/locate/jngse

Potential risk of H_2S generation and release in salt cavern gas storage

Christina Hemme*, Wolfgang van Berk

TU Clausthal, Institute of Disposal Research, Department of Hydrogeology, Leibnizstrasse 10, 38678 Clausthal-Zellerfeld, Germany

ARTICLE INFO

Article history:
Received 9 June 2017
Received in revised form
21 August 2017
Accepted 23 September 2017
Available online 9 October 2017

Keywords:
H_2S
Salt cavern gas storage
Bacterial sulfate reduction
Gas souring
Reactive transport modelling
PHREEQC

ABSTRACT

The storage of natural gas in salt caverns can entail the risk of H_2S generation, which in turn leads to gas pollution. H_2S is generated by bacterial sulfate reduction. The bacteria use aqueous $sulfate_{(aq)}$ as an electron acceptor to oxidize the dissolved hydrocarbons and generate sulfide. Anhydrite is available in the rock salt surrounding the cavern and acts as a $sulfate_{(aq)}$ source. The stored natural gas, with its main component, methane, is in solubility equilibrium with the brine and is additionally delivered by diffusion into the brine. The generated H_2S reaches the stored gas by outgassing from the brine. In this study, these processes are simulated by one- and three-dimensional hydrogeochemical diffusive mass transport models, which are based on equilibrium reactions for gas-water-rock interactions and kinetic reactions for sulfate reduction. Modelling results show that the greatest amount of H_2S is generated in the brine. The amount of generated $H_2S_{(g)}$ is mainly controlled by the amount of available $sulfate_{(aq)}$ as well as the rate of diffusion, which is coupled with the maximum operating live time of salt caverns. Additionally, the amount of generated and released $H_2S_{(g)}$ is sensitive to the chosen kinetic rate constant.

To ensure constant gas quality over time, the gas and the brine must be analyzed continuously and technical methods must be applied when the $H_2S_{(g)}$ concentration increases. According to the modelling results, $H_2S_{(g)}$ generation is inhibited by addition of dissolved ferrous iron to the brine. Dissolved ferrous iron reacts with sulfide-sulfur to form mackinawite ($FeS_{(s)}$) so that aqueous sulfide is no longer available for $H_2S_{(g)}$ generation. Another method is the addition of NaOH to increase the pH of the brine. Then, higher fractions of generated sulfide-sulfur are transformed to free $S^{2-}{}_{(aq)}$ instead of $H_2S_{(g)}$ and $H_2S_{(aq)}$.

1. Introduction

Natural gas is stored in salt caverns to balance the supply and demand of natural gas throughout the year. Salt caverns are highly qualified for hydrocarbon storage because of numerous physical properties and mechanical behaviors of the rock salt halite, like its self-healing forces and its impermeability below 300 m (Evans, 2008; Yang et al., 2013). However, Evans (2008) has stated that "there is a need to assess the safety record of previous and existing underground fuel storage facilities." One risk is the potential generation and release of gaseous hydrogen sulfide ($H_2S_{(g)}$) in natural gas storage systems. H_2S is toxic if inhaled, is aggressive towards storage facilities (Cord-Ruwisch et al., 1987; Kleinitz and Böhling, 2005), and can pose a threat to the environment (Reitenbach et al., 2015). The presence of H_2S can lead to corrosion of metallic iron under anaerobic conditions and to the precipitation of amorphous ferrous sulfide, which in turn may cause plugging (Cord-Ruwisch et al., 1987). Even more importantly, H_2S contaminates the stored gas and can affect the gas quality (Cord-Ruwisch et al., 1987). Therefore, in Germany, technical regulations determine that the concentration of 5 mg/m^3 $H_2S_{(g)}$ in stored gas must not be exceeded (DVGW, 2013).

There are considerable indications that $H_2S_{(g)}$ generation could be a potential risk in salt caverns used for gas storage. First, H_2S is observed in hydrocarbon reservoirs where it originates from sulfate reduction (Machel, 2001), either via abiotic reactions or via reactions catalyzed by bacteria. The abiotic reaction, so-called thermochemical sulfate reduction (TSR), is common in geological settings with temperatures ranging from 100 to 180 °C, while the bacterial sulfate reduction (BSR), occurs in low-temperature geological settings ranging from 0 °C to 60–80 °C (Ehrlich, 1990; Machel, 2001; Postgate, 1984). In some cases, BSR has been

* Corresponding author.
E-mail address: christina.hemme@tu-clausthal.de (C. Hemme).

https://doi.org/10.1016/j.jngse.2017.09.007

observed above 80 °C. Hyperthermophilic sulfate-reducing bacteria may live at temperatures up to 110 °C (Jorgensen et al., 1992). However, BSR does not necessarily occur in all hydrocarbon-bearing geosystems with temperatures below 80 or 110 °C. Otherwise, all hydrocarbon reservoirs below this temperature would be sour, meaning H_2S-bearing (Machel, 2001), and would display higher total sulfide concentrations in the aqueous and the gas phase. Therefore, in this study, we focus on salt caverns filled by natural gas and exposed to temperatures ranging from 50 to 80 °C. Our focal point is the formation of sulfide-sulfur (S(-II)) from sulfate-sulfur (S(+VI)) via BSR and the subsequent release of formed sulfide-sulfur (S(-II)) as $H_2S_{(g)}$ into the stored natural gas.

An additional indication of H_2S generation by BSR in salt caverns is the possible anaerobic oxidation of methane (AOM), which is observed in marine as well as in non-marine environments (Meulepas et al., 2010). In aqueous anoxic environments, sulfate-reducing bacteria (SRB) use sulfate as an electron acceptor to oxidize organic compounds and generate sulfide (Eq. (1)). This generated sulfide-S could be available as aqueous H_2S, $HS^-_{(aq)}$, and $S^{2-}_{(aq)}$ and gaseous H_2S. SRB use the produced energy from sulfate reduction to sulfide for cell growth (Cord-Ruwisch et al., 1987). The sulfate for BSR could be derived from the aqueous dissolution of calcium sulfide-sulfur mineral phases like gypsum $(CaSO_4[2H_2O])_{(s)}$ and anhydrite $(CaSO_4)_{(s)}$.

$$SO^{2-}_{4(aq)} + CH_{4(aq)} \xrightarrow{H_2O} H_2S_{(aq)} + CO^{2-}_{3(aq)} + H_2O \quad (1)$$

The increasing demand for storage capacity in salt caverns requires the utilization of less favorable salt formations, including inhomogeneous salt structures with larger proportions of insolubles like anhydrite layers (Schneider and Crotogino, 2010). Drilling operations and/or workover operations may lead to bacterial contamination of hydrocarbon reservoirs, or SRB populations may pre-exist in such reservoirs (Kleinitz and Böhling, 2005). The optimal growth temperature for SRB is 38 °C (Bernardez et al., 2013) at near-neutral pH conditions (Cord-Ruwisch et al., 1987). However, SRB also occur in more acidic environments of pH 3 (Tuttle et al., 1969) and pH 4 (Church et al., 2007).

Furthermore, BSR is observed in saline environments where high rates of sulfate reduction are measured (Kjeldsen et al., 2007). The activity of most SRB decreases if the Na^+/Cl^- concentrations are above 50–100 g/L (Cord-Ruwisch et al., 1987; Postgate, 1984; ZoBell, 1958) but activity of SRB is even found in salt lakes and brines near "salt saturation" (ZoBell, 1958). Even if these conditions are not the optimum for SRB growth, a few SRB tolerate the high salt (NaCl) concentrations and live near salt saturation (Cord-Ruwisch et al., 1987).

Additionally, $H_2S_{(g)}$ is detected in underground storage systems of town gas (Crotogino, 2016) and in underground gas storage in porous media (Kleinitz and Böhling, 2005). Furthermore, the activity of sulfate-reducing bacteria is observed in salt caverns filled by hydrogen gas. There, the SRB live in the sump and in the brine, generating biofilms at the cavern walls (Panfilov, 2016).

This study focuses on H_2S generation by bacterial sulfate reduction in a salt cavern that is described by one- and three-dimensional hydrogeochemical reactive transport models. It is based on thermodynamic equilibrium reactions for gas-water-rock interactions and kinetic reactions for sulfate reduction. The aims of this study are (1) to draw the attention of the possible risk of $H_2S_{(g)}$ pollution in salt caverns, (2) to clarify and quantify time-dependent $H_2S_{(g)}$ generation processes in salt caverns filled with natural gas, (3) to analyze the limiting factors for $H_2S_{(g)}$ generation and release in salt caverns, and (4) to identify technical methods to decrease or inhibit $H_2S_{(g)}$ generation and release.

2. Methodology

2.1. Modelling tools

The one- and three-dimensional reactive mass transport models are based on chemical-thermodynamically principles, the reaction kinetics of BSR and the principles of diffusive mass transport.

The modelling tool for the 1-D model in this study is the computer program PHREEQC version 3 provided by the U.S. Geological Survey. PHREEQC is based on an ion-association aqueous model and can simulate batch-reaction, speciation, inverse geochemical and one-dimensional transport calculations (Parkhurst and Appelo, 2013). The calculations are based on mass action laws including all species and their corresponding equilibrium constants. The activity coefficients of species are calculated by the Debye-Hückel equation. The equilibrium phases, mass-action equations, and equilibrium constants used in the model are shown in Table 1.

The computer program PHAST (version 3.3.7–11094), provided by the U.S. Geological Survey, is the modelling tool for the 3-D model. Using PHAST, multicomponent geochemical reactions, solute transport and groundwater flow can be simulated (Parkhurst and Charlton, 2010). The geochemical reactions in PHAST are simulated with PHREEQC and the flow and transport calculations are based on HST3D; both programs are embedded in PHAST (Parkhurst and Charlton, 2010). The results are visualized using the software Model Viewer (Hsieh and Winston, 2002). The combined application of PHREEQC/PHAST and the Model Viewer software enables the visualization of the temporal and spatial development of H_2S generation in salt cavern gas storages. Detailed information about PHREEQC and PHAST are given in Parkhurst and Appelo (2013) and Parkhurst and Charlton (2010).

The thermodynamic database; which includes all elements used in the model with their species (aq, s, g), mass-action equations, and equilibrium constants; is essential for modelling with PHREEQC and PHAST. The database used for 1-D and 3-D modelling is phreeqc.dat. A more suitable database for the high Na^+ and Cl^- concentrations and the high ionic strength in the model could be the Pitzer database (pitzer.dat), but pitzer.dat does not include Si-containing aqueous species, Al^{3+}, and silicate minerals, which are important factors when modelling H_2S generation in salt caverns. To validate that PHREEQC (using phreeqc.dat) produces correct results, even under high Na^+ and Cl^- concentrations and high ionic strength, the salt solubility in PHREEQC (using phreeqc.dat) is compared with salt solubility data from literature. In Zimmermann et al. (1986), the solubility of Na^+/Cl^- is given in dependence of the

Table 1
Equilibrium phases, mass-action equations, and equilibrium constants (log K, at 25 °C and 1 bar). Data are from phreeqc.dat, except for $CH_{4(g)}$, $H_2S_{(g)}$, $N_{2(g)}$ which are from llnl.dat (Parkhurst and Appelo, 2013).

Equilibrium phase	Equilibrium reaction	log K
Halite	$NaCl = Cl^- + Na^+$	1.570
Anhydrite	$CaSO_4 = Ca^{2+} + SO_4^{2-}$	−4.39
Siderite	$FeCO_3 = Fe^{2+} + CO_3^{2-}$	−10.89
Quartz	$SiO_2 + 2H_2O = H_4SiO_4$	−3.98
Barite	$BaSO_4 = Ba^{2+} + SO_4^{2-}$	−9.97
Pyrite	$FeS_2 + 2H^+ + 2e^- = Fe^{2+} + 2HS^-$	−18.479
Dolomite	$CaMg(CO_3)_2 = Ca^{2+} + Mg^{2+} + 2CO_3^{2-}$	−17.09
Mackinawite	$FeS + H^+ = Fe^{2+} + HS^-$	−4.648
Sulfur[a]	$S + 2H^+ + 2e^- = H_2S$	4.882
Calcite	$CaCO_3 = CO_3^{2-} + Ca^{2+}$	−8.48
$CH_{4(g)}$	$CH_4 = CH_4$	−2.8502
$CO_{2(g)}$	$CO_2 = CO_2$	−1.468
$H_2S_{(g)}$	$H_2S = H^+ + HS^-$	−7.9759
$N_{2(g)}$	$N_2 = N_2$	−3.1864

[a] Sulfur = elemental sulfur.

temperature. At 40 °C, 36.42 g Na^+/Cl^- (halite) dissolves in 100 g water (= 6.23 mol/kgw for Na^+ and Cl^-). This measurement is consistent with the results of Na^+/Cl^- solubility in PHREEQC using phreeqc.dat (= 6.32 mol/kgw for Na^+ and Cl^-), with the discrepancy that the temperature in the model is 50 °C. $NaCl_{(solid)}$ solubility data in pure water at different temperatures from literature (experimental data) are compared with modelled data (PHREEQC with phreeqc.dat) and are summarized in Table 2.

2.2. Model setup

Salt caverns are divided into three parts (Fig. 1): the stored gas at the top, which takes up the largest volume; the brine in the middle, with a thickness of only a few meters; and the sump at the bottom, which can occupy one third of the total cavern volume (Bérest and Brouard, 2003; Panfilov, 2016). The sump is composed of insoluble residues (Evans, 2008) and a residual pore-filling aqueous solution that is not discharged after leaching (Panfilov, 2016). Due to technical reasons, residual brine is situated above the sump (Haddenhorst, 1989). This brine is in solubility equilibrium with the gas stored above (Fontenot, 1981; Réveillère et al., 2016) and the surrounding mineral phases of the rock salt formation.

The initial gas composition in the model is based on data from DVGW (2013). The main component is $CH_{4(g)}$ (partial pressure of CH_4 (ρCH_4) = 178.128 atm), with minor amounts of $N_{2(g)}$ ($\rho N_{2(g)}$ = 1.548 atm), $CO_{2(g)}$ ($\rho CO_{2(g)}$ = 0.324 atm), and $H_2S_{(g)}$ ($\rho H_2S_{(g)}$ = 0.00018 atm), hereinafter called “initial gas”. For the sake of simplicity, the partial pressure is assumed to be equal to the fugacity f ($\rho = f$). The total gas pressure is 180 atm, and the temperature in the salt cavern is 50 °C.

The mineralogical composition of the sump and the brine are characterized by the composition of the surrounding rock salt formation and the solution used for leaching. The mineralogical composition of the rock salt formation is based on data from Kyle and Posey (1991) and is shown in Table 3. For leaching, the chemical composition of groundwater taken from a ca. 20 m depth quaternary aquifer from Lower Saxony, northern Germany (NLWKN, 2015) is used (Table 4).

A salt cavern with a height of 350 m, divided into 300 m stored gas, 2 m brine, and 48 m sump, is assumed. The focal point of the model is the brine-gas interface and the upper meters of the sump (Fig. 1). Therefore, the model is divided into a column of 8 cells, with a cell height of 1.0 m each (in the z-direction). The boundary at the upper end of the column represents a constant amount of stored gas. At the lower end of the column, the boundary condition is defined as diffusive flux. The only mass transport in this model is molecular diffusion of all aqueous species. One diffusion coefficient for all aqueous species of 5.0×10^{-9} m^2/s is used. Cell 1 delivers CH_4 (C(-4)) continuously by diffusion. Cell 2 is located at the brine-gas interface, cell 3 in the brine, and cells 4–8 in the sump. Each cell is defined by specific mineralogical and hydrochemical properties. The brine and residual aqueous solution compositions are calculated in separated batch models with PHREEQC (Table 4).

The brine (cell 2) is composed of the solution used for leaching and is equilibrated with the mineralogical composition of the rock salt and the initial gas composition. It has a total volume of 1 L, which is equivalent to 1 kg of pure water (kgw). The gas phase in cell 2 has a total volume of 270,000 L (based on the model height for gas of 300 m, a base area of 0.005 m^2, and a pressure of 180 atm) and represents the stored gas volume at 180 atm under the assumed salt cavern design. For modelling purposes, this gas is a tracer gas with the same chemical properties as $CH_{4(g)}$. It is used instead of $CH_{4(g)}$ because CH_4 is induced and used as reactant in the calculation kinetics. The partial pressure of the tracer gas is equivalent to the total pressure in the cavern so that the generated H_2S is released as gas bubbles. The brine in cell 3 is composed of the solution used for leaching equilibrated with the mineralogical composition of the rock salt but without being in equilibrium with a gas phase. However, the possibility of $H_2S_{(g)}$ outgassing is assumed, and calcite, mackinawite, and elemental sulfur are potential secondary phases that may form at saturation.

The residual aqueous solution in the sump (cells 4–8) is composed of the solution used for leaching equilibrated with the mineralogical composition of the rock salt formation (Table 4). An initial porosity of 20% is assumed in the sump. The amount of each mineral phase is calculated in moles per kg of pore water by considering the specific density of each mineral phase (g/cm^3) and is summarized in Table 3. Additionally, calcite, mackinawite, and elemental sulfur are potential secondary phases that may form at saturation. No gas phase is available, but the possibility of $H_2S_{(g)}$ outgassing is assumed in all cells.

The oxidation of methane by sulfate in the model system is kinetically controlled. The sulfate reduction rate of 6.46×10^{-10} mol kgw^{-1} s^{-1} at 55 °C is derived from Adams et al. (2013). The initial amount of $CH_{4(aq)}$ in the brine is 0.027 mol/kgw. That corresponds to the maximum amount of $CH_{4(g)}$ in the brine under assumed solubility-equilibration-conditions at a $pCH_{4(g)}$ of 180 atm and 50 °C. A separate transport model provides the initial amount of $CH_{4(g)}$ in the sump for the kinetic calculation. This amount corresponds to the maximum available amount of $CH_{4(g)}$ that could be delivered to the sump by diffusion in a timeframe of 30 years (because the typically operating life of a salt cavern is 30 years). In 30 years, 0.007 mol/kgw CH_4 is available in the first meter of the sump, 0.004 mol/kgw CH_4 in the second meter, 0.003 mol/kgw CH_4 in the third meter and 0.001 mol/kgw CH_4 in the fourth meter of the sump.

The diffusive mass fluxes are calculated by multiplying diffusivity with tortuosity. Diffusivity is defined by the coefficient of molecular diffusion of aqueous species in dilute solutions without a porous matrix (Fu et al., 2016). A diffusivity of 10^{-9} m^2 s^{-1} for all aqueous species involved in the model is assumed. Tortuosity describes the relation of effective diffusion mass fluxes in a porous medium to ideal diffusion mass fluxes in dilute solutions without a rock matrix and varies between 0.0 and 1.0. To show the influence of the diffusive mass transport on the modelling results, the values of tortuosity in different modelling scenarios are systematically varied (Section 3.2.4).

Alternating operating phases characterize the total gas pressure in a salt cavern, divided into a minimum pressure phase, injection pressure phase, maximum pressure phase, and production pressure phase (Wang et al., 2015). The pressure is varied between a minimum of 60 atm and a maximum of 180 atm in different modelling scenarios (Section 3.2.1). Because PHAST is not capable of calculating the pressure dependence of solubility equilibrium constants for minerals, gases and aqueous species, the pressure dependence is simulated in a separate model using the software PHREEQC and the database phreeqc.dat (Parkhurst and Appelo, 2013).

Table 2
$NaCl_{(solid)}$ solubility [mol/kgw] in pure water at different temperatures from literature (experimental data) and modelled data. The database phreeqc.dat is used in the PHREEQC model.

Solubility $NaCl_{(solid)}$ - Data	0 °C	20 °C	40 °C	60 °C
	[mol/kgw]	[mol/kgw]	[mol/kgw]	[mol/kgw]
Zimmermann et al. (1986)	6.09	6.13	6.23	6.34
PHREEQC modelling	6.00	6.10	6.24	6.39

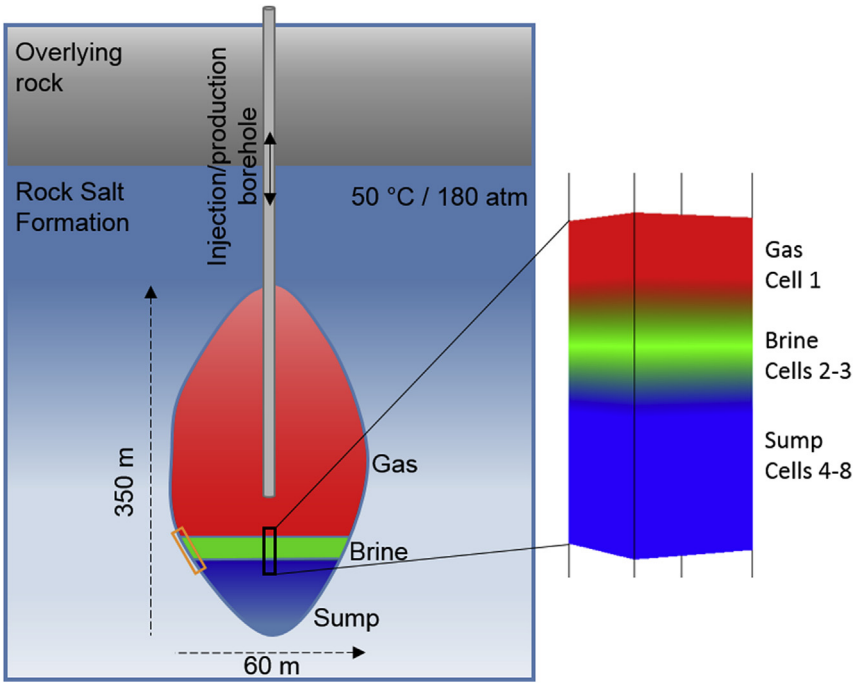

Fig. 1. System sketch of the model. Black box = reference scenario, orange box = alternative scenario. article).

Table 3
Initial mineralogical composition of the rock salt formation used for the sump with a porosity of 20%. The data are modified after Kyle and Posey (1991). Mackinawite, elemental sulfur, and calcite are potential secondary phases which may form at saturation.

Primary mineral phases	Weight percent [wt%]	Amount [mol/kgw]
Halite	97.0	144.62
Anhydrite	2.75	1.76
Siderite	0.05	0.04
Quartz	0.05	0.07
Barite	0.05	0.02
Pyrite	0.05	0.04
Dolomite	0.05	0.02

Table 4
Groundwater composition used for leaching (NLWKN, 2015), initial composition of the brine, and the aqueous solution in the sump.

	Groundwater	Solution in the sump	Brine
pH	6.4	8.2	5.7
Temperature [°C]	10.1	50.0	50.0
Elements	Concentration [mol/kgw]	Concentration [mol/kgw]	Concentration [mol/kgw]
Ba	-[a]	8.136e-07	9.097e-07
C	-[a]	2.901e-05	7.077e-03
Ca	1.622e-03	5.488e-02	6.333e-02
Cl	8.380e-04	6.306e+00	6.310e+00
Fe	1.522e-06	2.257e-03	1.415e-03
K	1.010e-04	1.010e-04	1.010e-04
Mg	3.150e-04	1.464e-02	1.315e-03
Mn	9.100e-07	9.100e-07	9.100e-07
N_{tot}[b]	1.152e-03	1.152e-03	3.008e-04
Na	7.050e-04	6.306e+00	6.310e+00
O (0)	6.600e-05	-[a]	-[a]
P	4.840e-07	4.840e-07	4.840e-07
S_{tot}[c]	8.540e-04	7.108e-02[c]	6.262e-02[c]
Si	2.560e-04	5.242e-05	3.368e-02

[a] Not presented.
[b] N_{tot}: summed concentration of aqueous N(-III), N(+III), N(+V) species.
[c] S_{tot}: summed concentration of aqueous S(+VI) and S(-II) species.

3. Results and discussion

3.1. H_2S generation and release - reference scenario

The results of the modelled reference scenario show that $CH_{4(g)}$ dissolves from the stored gas into the brine (at the brine-gas interface), according to the pressure/temperature conditions. $CH_{4(aq)}$ diffuses through the brine and the sump, where $SO_4^{2-}{}_{(aq)}$-ions are available for BSR. The $SO_4^{2-}{}_{(aq)}$-ions result from anhydrite dissolution and diffuse from the sump to the brine-gas interface, where $CH_{4(aq)}$ is available. The diffusive mass transport is induced by concentration gradients and causes a complex web of hydro-geochemical reactions and processes, including BSR. Modelling results indicate that $H_2S_{(g)}$ generation in salt caverns by bacterial sulfate reduction mainly occurs on the diffusive path where methane and sulfate meet and react with each other. The highest total H_2S concentrations are at this meeting point. Therefore, how much $H_2S_{(g)}$ is generated over time depends on diffusion as well as on the reaction kinetic of BSR, both depending on temperature and/or pressure. Fig. 2 shows the results of the 3-D model and indicates the location of $H_2S_{(g)}$ generation, as well as increasing $H_2S_{(g)}$ concentration with ongoing time and BSR. The maximum amount of generated $H_2S_{(g)}$ is 0.0515 mol/kgw (= 6.50 mg/m^3 $H_2S_{(g)}$) after 30 years, in total.

Comparing the results of the reference scenario modelled in 3-D in PHAST to the results of the reference scenario modelled in 1-D in PHREEQC, slight differences are identifiable. After 30 years, 7.19 mg/m^3 $H_2S_{(g)}$ are generated in PHREEQC and 6.50 mg/m^3 $H_2S_{(g)}$ are generated in PHAST. Additionally, the results of the 1-D model show that $H_2S_{(g)}$ is released into the stored gas and how much is released after 30 years and the results of the 3-D model show the location where $H_2S_{(g)}$ is generated. Furthermore, PHAST includes flow and transport calculations (including parameters like tortuosity and dispersivity). Nevertheless, the differences are small and the chemical processes are the same because the geochemical reactions in PHAST are simulated with PHREEQC. The following results refer to the 1-D model to make them comparable with the results of the following scenarios (Section 3.2). Another reason to use PHREEQC is the higher interest for industry in $H_2S_{(g)}$ concentration in the stored gas than the point where it is generated.

H_2S is formed as a gas bubble in the brine and released into the stored gas above if the sum of the partial pressure of all dissolved gases$_{(aq)}$ is greater or equal to the total gas pressure in the stored gas. At 50 °C and 180 atm, a total of 7.19 mg/m^3 $H_2S_{(g)}$ is released into the stored gas after 30 years. The value lies above the allowed limit of 5 mg/m^3 (defined by DVGW (2013)).

Aqueous sulfate is available in the brine from anhydrite dissolution (during leaching and operation) and is additionally delivered by diffusion from the sump. Furthermore, the dissolution of anhydrite contributes $Ca^{2+}{}_{(aq)}$ into the brine and, in consequence, calcite precipitates. In 30 years, 0.035 mol/kgw calcite precipitates at the brine-gas interface and buffers the effects of BSR on the pH of the brine. Therefore, the increase in the pH of the brine over 30 years is small (from 5.7 to 6.1). S(-II), a product of BSR, reacts with the available aqueous Fe(+II) and mackinawite precipitates (0.004 mol/kgw in 30 years), inhibiting H_2S generation. Another possible reaction is S(-II) with Fe(+II) to form pyrite. Using pyrite instead of mackinawite as a potential secondary phase, the amount of generated $H_2S_{(g)}$ is smaller (5.96 mg/m^3). However, the stabilities of pyrite and/or mackinawite at this pressure and temperature conditions are not identified. Furthermore, a small amount of pure water (H_2O) forms as a product of BSR with a maximum of 0.0004 kg/kgw. Elemental sulfur is included in the model as a potential secondary phase but does not precipitate, even if pyrite and mackinawite are not included as potential secondary phases.

The reference scenario considers the inner part of the cavern and neglects the cavern wall with its equilibrium phases of the rock salt formation which are in contact with the brine (Fig. 1, orange box). To cover this part of the salt cavern, an alternative scenario is modelled. Modelling results show that $H_2S_{(g)}$ generation at the cavern wall is less intensive (5.15 mg/m^3) than in the part of the cavern that is not in contact with the cavern wall (the reference scenario, where no equilibrium phases are available in the brine). This is tested by adding the same equilibrium phases used in the sump to the brine. Conceptually, a water-to-rock ratio equivalent to a theoretical porosity of 80% is assumed. The decrease in $H_2S_{(g)}$ generation can be explained with the occurrence of siderite, which is part of the initial rock salt formation. As long as siderite is available, S(-II) is bound to newly formed mackinawite and inhibits $H_2S_{(g)}$ generation stronger than in the reference scenario. The initial amount of 0.001 mol/kgw siderite is completely dissolved in less than 3 years. Furthermore, more calcite precipitates (0.06 mol/kgw), which more strongly buffers the effect of BSR on the pH, so that the pH increase is smaller compared to the $H_2S_{(g)}$ generation in the center of the cavern (from 5.7 to 5.8). After less than 12 years, the available anhydrite at the brine-gas interface (cell 2) is

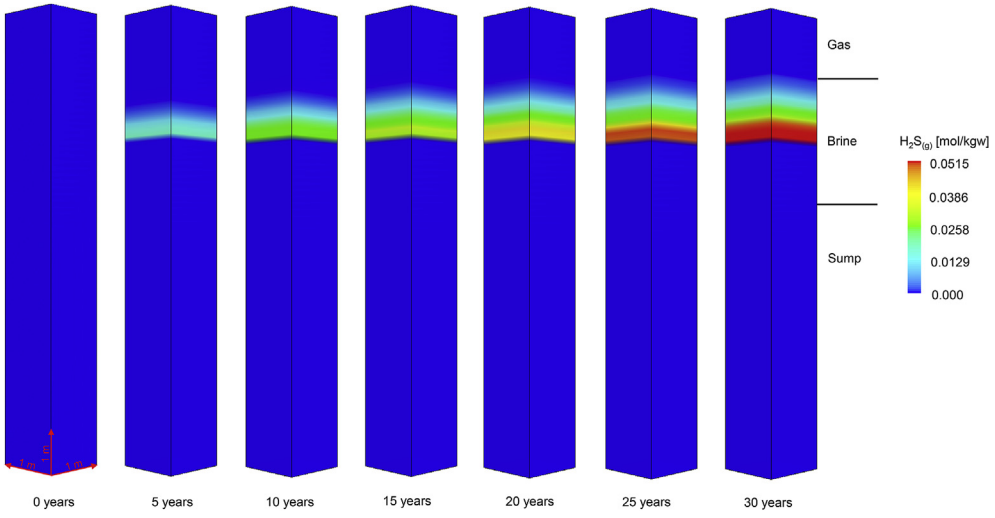

Fig. 2. $H_2S_{(g)}$ generation and increasing $H_2S_{(g)}$ amount with ongoing time and bacterial sulfate reduction.

completely dissolved. Furthermore, irreducible water is available in the surrounding rock salt formation so that diffusional transport of $CH_{4(aq)}$ and available $SO_4^{2-}{}_{(aq)}$-ions is possible even at the cavern wall in the part of the cavern where the gas is stored. Consequently, $H_2S_{(g)}$ could be generated even there.

3.2. Factors influencing $H_2S_{(g)}$ generation and release

Generic model scenarios show the consequences of varying conditions in salt caverns on the H_2S generation and release. In the following Sections, 3.2.1–3.2.4, the impacts of different factors are analyzed.

3.2.1. Gas pressure changes in salt cavern gas storages

Special consideration is given to the effect of pressure changes in the cavern as a consequence of gas injection, storage, and production phases. This scenario is based on Wang et al. (2015) where a 1-year cycle is assumed, divided into 3 months of storage at minimum pressure (60 atm), 3 months of injection (120 atm, as a "mean" between 60 atm and 180 atm), 3 months of storage at maximum pressure (180 atm), and 3 months of production (120 atm). The modelling tool for this scenario is PHREEQC, with the database phreeqc.dat where the pressure-dependent mass-action law constants for the equilibrium reactions of the involved gaseous, aqueous, and solid species are included. Fig. 3a shows $H_2S_{(g)}$ generation and release versus pressure.

After the first 3 months of storage at maximum pressure, a total of 0.59 mg/m^3 $H_2S_{(g)}$ is generated and released. During each of the subsequent phases (3 months of production, 3 months of storage at low pressure, and 3 months of injection), 0.3 mg/m^3 $H_2S_{(g)}$ is generated and released. The cycle starts again with a high-pressure storage phase where only 0.3 mg/m^3 $H_2S_{(g)}$ is generated and released (Fig. 3a). The high amount of $H_2S_{(g)}$ (0.59 mg/m^3) generated and released in the first maximum pressure phase can be explained with the higher amount of aqueous sulfate in the brine at the beginning of storage, which results from anhydrite dissolution during leaching. The amount of aqueous sulfate available from leaching in the brine decreases with ongoing BSR, but additional aqueous sulfate is delivered by diffusion from the sump, where anhydrite is still available. When the amount of sulfate in the brine is consumed, the sulfate is delivered only by diffusion. Therefore, the change in pressure conditions has minor influence on $H_2S_{(g)}$ generation and release, but diffusion of dissolved sulfate and dissolved methane through the brine is the limiting factor. To confirm these results, additional modelling scenarios were performed with an extended range of pressure conditions. Modelling results show that even under very low-pressure (25 atm) and high-pressure conditions (300 atm) the amount of generated and released $H_2S_{(g)}$ is nearly constant at 0.3 mg/m^3 (0.2999 mg/m^3 at 25 atm and 0.30002 mg/m^3 at 300 atm).

3.2.2. Natural gas composition

The chemical composition of the stored natural gas can differ. An alternative gas composition, based on data from the DVGW (2013), with 175.032 atm ρCH_4, 1.476 atm ρN_2, 3.492 atm ρCO_2, and 0.000288 atm ρH_2S is used to show the influence of the initial gas composition on $H_2S_{(g)}$ generation and release. The results of the 1-D model (in PHREEQC) show a slight increase in $H_2S_{(g)}$ generation and release from 7.19 mg/m^3 $H_2S_{(g)}$ (reference scenario) to 7.22 mg/m^3 $H_2S_{(g)}$ using this alternative gas composition (Fig. 3b). The pH decreases to 5.9 from 6.1 in the reference scenario. The amount of precipitated calcite increases slightly (from 0.035 mol/kgw in the reference scenario to 0.037 mol/kgw) but the amount of precipitated mackinawite is nearly constant (0.004 mol/kgw in 30 years). Generally, the initial gas composition can influence the final $H_2S_{(g)}$ generation and release, but in this case, the effect is minor.

3.2.3. Kinetic rate constants

The kinetic rate constant of BSR is an important factor controlling $H_2S_{(g)}$ generation and release. The rate constant is varied from an initial 6.46×10^{-10} mol kgw^{-1} s^{-1} (based on Adams et al. (2013)) to 1.04×10^{-09} mol kgw^{-1} s^{-1} (based on Kallmeyer and Boetius (2004)) and 5.95×10^{-08} mol kgw^{-1} s^{-1} (based on Timmers et al. (2016)). All rate constants used apply to temperature and pressure conditions comparable to salt cavern conditions. The presented results are based on the 1-D model in PHREEQC. As shown by Fig. 3c, with increasing rate constant the $H_2S_{(g)}$ generation and release increases. The elevated rate constant of 1.04×10^{-09} mol kgw$^-$ s^{-1} causes an increase from 7.19 to 7.59 mg/m^3 $H_2S_{(g)}$ and the rate constant of 5.95×10^{-08} mol kgw^{-1} s^{-1} an increase to 8.88 mg/m^3 $H_2S_{(g)}$ after 30 years. The results show that by varying the rate constant, other interconnected reactions are affected as well. Comparing the results of the reference scenario to the results of the scenario with the rate constant of 5.95×10^{-08} mol kgw^{-1} s^{-1}, the following changes are observable at the brine-gas interface: the amount of the secondary phase calcite decreases slightly from 0.035 mol/kgw to 0.032 mol/kgw and mackinawite formation increases from 0.0038 mol/kgw to 0.0047 mol/kgw (whereas the pH is constant at 6.1). In consequence, the variations in the amount of generated and released $H_2S_{(g)}$ indicate that it is important to determine the kinetic rate constants at elevated levels of temperature of 50 °C and other relevant site-specific cavern conditions as accurately as possible. However, doubling the rate constant does not double the amount of generated and released $H_2S_{(g)}$ because diffusion is the main limiting factor.

3.2.4. Tortuosity

Another influencing factor is the tortuosity, included in the 3-D PHAST model. With increasing tortuosity in brine and sump (from 0.001 to 0.01, 0.1 and 1.0), bacterial sulfate reduction increases due to more effective diffusive transport of $CH_{4(aq)}$ and $SO_4^{2-}{}_{(aq)}$. Therefore, the maximum value of generated $H_2S_{(g)}$ increases from 2.17 mg/m^3 (tortuosity of 0.001) to 7.98 mg/m^3 (tortuosity of 1.0; Fig. 3d) after 30 years. The higher the tortuosity, the lower the pH (from pH 9.5 with a tortuosity of 0.001 to pH 8.2 with a tortuosity of 1.0). Furthermore, the amount of precipitated calcite increases with increasing tortuosity (from 0.02 mol/kgw to 0.05 mol/kgw) and at higher tortuosity, intensified anhydrite dissolution is identified in the sump. The lower BSR rate at low tortuosity influences the amount of precipitated mackinawite, which is smaller at a tortuosity of 0.001 (0.002 mol/kgw) than at tortuosity of 1.0 (0.003 mol/kgw). The most significant difference in the amount of generated $H_2S_{(g)}$ is identifiable from a tortuosity of 0.001–0.01 (Fig. 3d). The differences in $H_2S_{(g)}$ generation from the tortuosity of 0.01–0.1 and to 1.0 are minor. These results also indicate that diffusion of dissolved methane and dissolved sulfate through the brine is the major limiting factor.

3.3. Inhibition of $H_2S_{(g)}$ generation and release in salt caverns

If the $H_2S_{(g)}$ concentration in the stored gas exceeds the limit of 5 mg/m^3 (DVGW, 2013), the stored gas is polluted and cannot be used anymore. Therefore, additional modelling scenarios show three possible methods to inhibit $H_2S_{(g)}$ generation and release. Generally, salt caverns should be constructed in rock salt formations with low amounts of anhydrite and other sulfate sources (e.g., gypsum). However, with increasing demand for storage capacity in salt structures, this is not always possible. In case the geogenic conditions favor $H_2S_{(g)}$ generation, as a first method a preventative measure should be applied. In this measure, $Fe(+II)_{(aq)}$ (dissolved

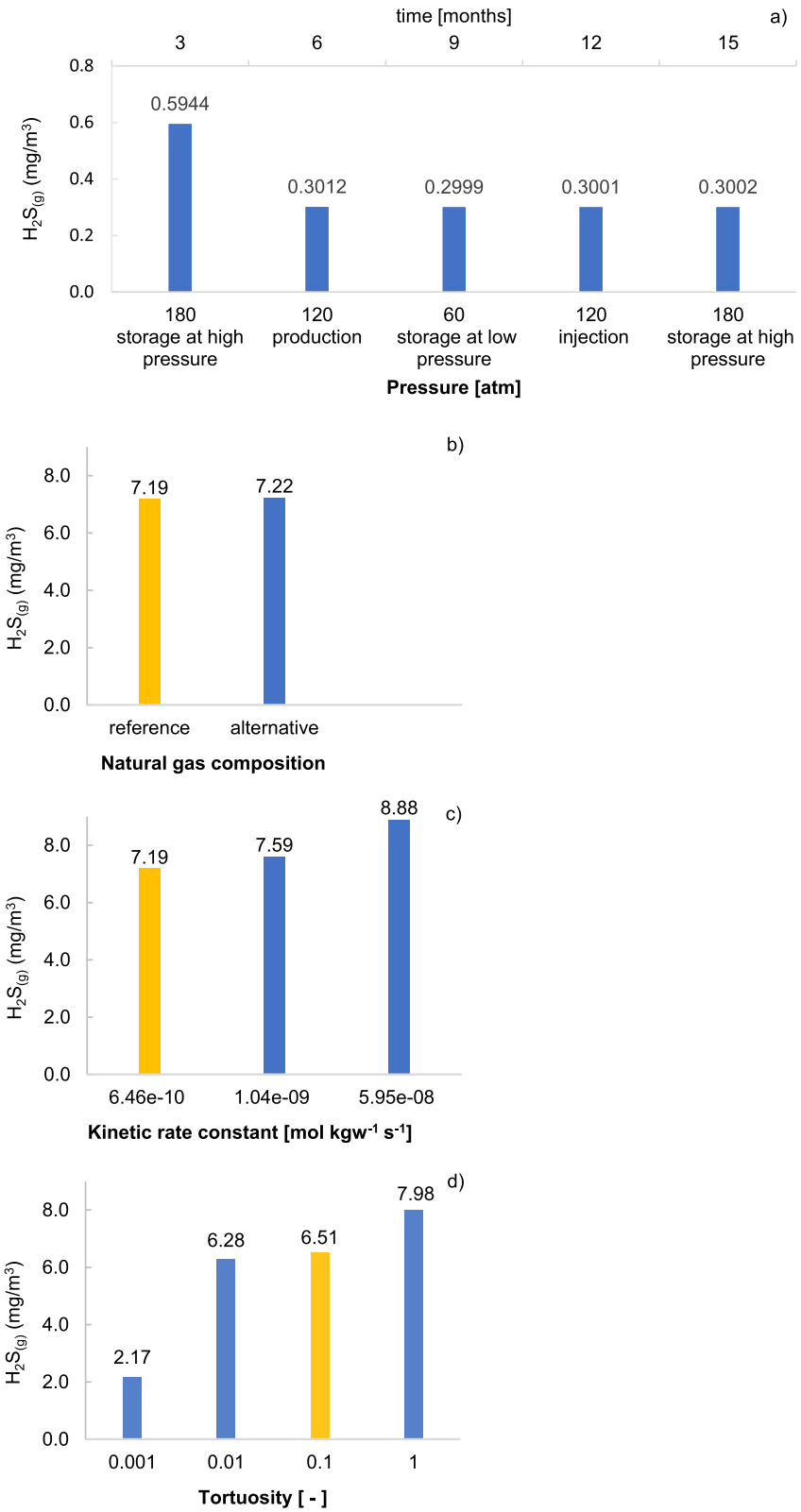

Fig. 3. $H_2S_{(g)}$ generation influenced by a) pressure changes (after 3 months) b) stored gas composition (reference = typical composition of natural gas from Russia, alternative = typical composition of natural gas from the North Sea (after 30 years) c) kinetic rate constant (after 30 years) d) tortuosity (after 30 years). $H_2S_{(g)}$ in mg/m^3 in the stored gas. Yellow = reference scenario, blue = modified parameters. a), b), and c) are modelled 1-D in PHREEQC, and d) is modelled 3-D in PHAST. (For interpretation of the references to colour in this figure legend, the reader is referred to the web version of this article).

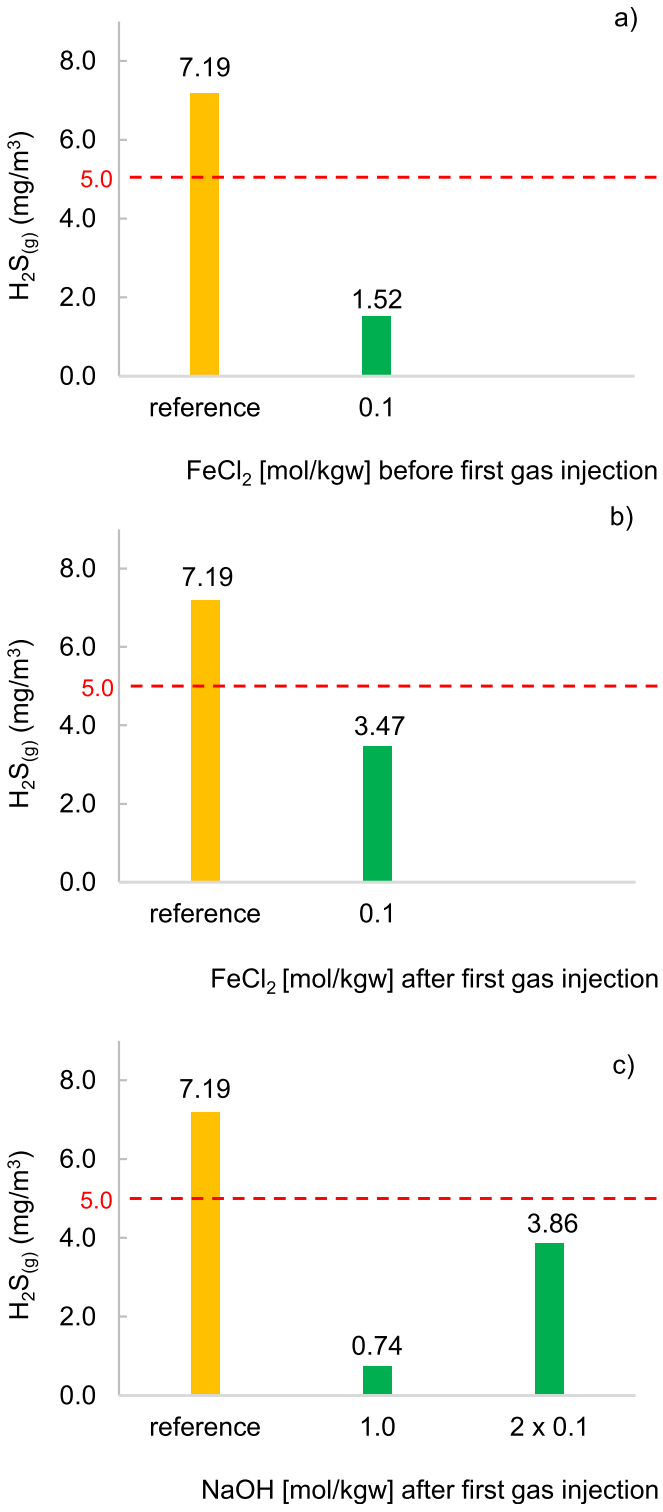

Fig. 4. $H_2S_{(g)}$, in mg/m^3, in the stored gas after 30 years. Inhibition of $H_2S_{(g)}$ generation and release by addition of a) $FeCl_2$ before first gas injection, b) $FeCl_2$ after gas injection c) 1.0 mol/kgw NaOH after 5 years of storage, and 0.1 mol/kgw NaOH after 5 years and after 10 years of storage to the brine. Reference is without any inhibition methods. Yellow = reference scenario, green = inhibition factors. Red line = maximum allowed $H_2S_{(g)}$ concentration in stored gas (defined by DVGW, 2013). (For interpretation of the references to colour in this figure legend, the reader is referred to the web version of this article).

$FeCl_2$) is added to the brine directly after leaching, before the first gas injection, and inhibits the $H_2S_{(g)}$ generation. The modelling results show a decrease in $H_2S_{(g)}$ generation from 7.19 mg/m^3 in the reference scenario to 1.52 mg/m^3. This can be explained by the higher amount of available Fe(+II), which reacts with aqueous sulfide to form mackinawite so that aqueous sulfide is no longer available for $H_2S_{(g)}$ generation (Fig. 4a). The amount of precipitated mackinawite increases from 0.004 mol/kgw (in the reference scenario) to 0.09 mol/kgw in the operating time of 30 years. The minimum concentration of $FeCl_2$ that must be added before the first gas injection to decrease the amount of generated $H_2S_{(g)}$ below the allowed limit of 5 mg/m^3 is 0.025 mol/kgw (assuming a homogeneous distribution of the injected $FeCl_2$).

Two inhibition methods could be used when an increase in $H_2S_{(g)}$ is detected in the stored gas. One method is to add $Fe(+II)_{(aq)}$ (dissolved $FeCl_2$) to the brine after first gas injection. The modelling results show that the available aqueous sulfide reacts with aqueous ferrous iron, and mackinawite precipitates. When adding 0.1 mol/kgw $FeCl_2$ after 5 years of storage, a total of only 3.47 mg/m^3 $H_2S_{(g)}$ is released after 30 years (Fig. 4b). The pH decreases from 6.1 to 5.8, less calcite precipitates (from 0.035 to 0.008 mol/kgw), and mackinawite precipitation increases strongly from 0.004 to 0.05 mol/kgw. The addition of 0.05 mol/kgw $FeCl_2$ after first gas injection is sufficient enough to reduce the $H_2S_{(g)}$ concentration just below the allowed limit of 5 mg/m^3 (assuming a homogeneous distribution of the added $FeCl_2$).

Another inhibition method is the addition of NaOH to the brine. Modelling results show that this method increases the pH and inhibits $H_2S_{(g)}$ generation. The pH influences the speciation type of the generated sulfide according to the mass action laws (included in the database phreeqc.dat). At neutral pH, most of the sulfide is available as H_2S and HS^-. In higher pH environments, HS^- and S^{2-} predominate, and at low pH, hydrogen sulfide occurs as H_2S. Therefore, when increasing the pH by addition of NaOH, more S^{2-} is generated (at constant S^{2-} in total), and gas pollution by $H_2S_{(g)}$ is inhibited. When 1.0 mol/kgw NaOH is added after 5 years of storage, the total amount of generated $H_2S_{(g)}$ after 30 years decreases to 0.74 mg/m^3 (Fig. 4c). The pH increases from 6.1 (in the reference scenario) to 11.5, calcite precipitation increases from 0.035 to 0.09 mol/kgw, and less mackinawite precipitates (from 0.004 to 0.002 mol/kgw). Another possibility is the addition of 0.1 mol/kgw NaOH after 5 years of storage and repetition of the same input after 10 years of storage. With these conditions, the total amount of generated $H_2S_{(g)}$ decreases to 3.86 mg/m^3 after 30 years (Fig. 4c). By addition of only 0.13 mol/kgw NaOH after 5 years of storage the $H_2S_{(g)}$ concentration is reduced to 4.99 mg/m^3. This amount is the minimum amount of NaOH that is needed to reduce the $H_2S_{(g)}$ concentration below the allowed concentration of 5 mg/m^3 under assumed storage conditions and homogenous distribution of added NaOH.

To ensure constant gas quality over time, the gas and brine must be analyzed continuously and the inhibition methods must be applied when the $H_2S_{(g)}$ concentration increases. Therefore, $H_2S_{(g)}$ measurements and monitoring in the gas as well as in the brine could be used as an early warning system. The application of sulphide scavengers is widely adopted in the oil and gas industry. Amosa et al. (2010) summarized the different scavenger technologies from copper-base scavengers to zinc-base scavengers and up to iron-base scavengers (among others). Less attention has been paid on the application of scavengers in underground gas storage systems especially in salt cavern gas storages. Some authors suggest to decrease the bacterial activity in the underground gas storage in porous media by “simple substitution” of products like heptamethyl nonane, dioxin, furan (Kleinitz and Böhling, 2005). They focus on procedures which prevent bacterial growth. However, the here presented study focuses on hydrogeochemical methods to decrease the generation and release of $H_2S_{(g)}$ in salt cavern gas

storage systems and on the quantitative description of the amount of $FeCl_2$ or NaOH that must be added to decrease the $H_2S_{(g)}$ concentration in the stored gas below the allowed limit of 5 mg/m^3 (defined by DVGW, 2013).

4. Conclusion

This study indicates that $H_2S_{(g)}$ generation and related pollution of the stored gas are risks in salt caverns. With increasing demand for storage capacity in salt caverns, the use of less favorable salt formations will increase, and the potential risk of $H_2S_{(g)}$ generation and release will rise. $H_2S_{(g)}$ in salt caverns is generated by bacterial sulfate reduction. The amount of available sulfate in the rock salt formation and diffusional transport are the main limiting factors of this process. The kinetic rate constant for bacterial sulfate reduction influences the amount of generated and released $H_2S_{(g)}$. Therefore, determining the kinetic rate constants at elevated levels of temperature and other relevant cavern conditions as accurately as possible is required. Experimental procedures to determine kinetic rate constants under consideration of site-specific conditions are presented e.g. by Adams et al. (2013), Jakobsen and Postma (1994), Timmers et al. (2016), Kallmeyer and Boetius (2004). Changing pressure conditions during injection, storage, and production phases has a minor influence on generated $H_2S_{(g)}$. Furthermore, the composition of the stored natural gas can influence $H_2S_{(g)}$ generation and release. The tortuosity effects the amount of generated $H_2S_{(g)}$, but the diffusion of dissolved methane and dissolved sulfate through the brine dominates this factor. In case of a site-specific model, the tortuosity can be roughly estimated by empirical equations based on petrophysical rock properties. Examples are given by Attia (2005), Shen and Chen (2007), Ewing et al. (2010), Ghassemi and Pak (2011).

Different hydrogeochemical methods inhibit $H_2S_{(g)}$ generation and release in salt caverns. One method is a prevention measure that could be applied before first gas injection if geogenic conditions favor $H_2S_{(g)}$ generation. In that method, $FeCl_2$ is added to the brine directly after leaching. Two further technical methods should be used for the inhibition of $H_2S_{(g)}$ generation, if during the time of storage an increase of $H_2S_{(g)}$ is observed in the gas or brine. The addition of aqueous $FeCl_2$ to the brine after gas injection leads to a reduction of $H_2S_{(g)}$ generation because the available aqueous sulfide reacts with the aqueous ferrous iron and mackinawite precipitates. Alternatively, NaOH could be added to the brine. This method increases the pH and inhibits $H_2S_{(g)}$ generation because the pH influences the speciation type of generated sulfide.

Acknowledgements

This research did not receive any specific grant from funding agencies in the public, commercial, or not-for-profit sectors.

References

Adams, M.M., Hoarfrost, A.L., Bose, A., Joye, S.B., Girguis, P.R., 2013. Anaerobic oxidation of short-chain alkanes in hydrothermal sediments: potential influences on sulfur cycling and microbial diversity. Front. Microbiol. 4 (110) https://doi.org/10.3389/fmicb.2013.00110.

Amosa, M.K., Mohammed, I.A., Yaro, S.A., 2010. Sulphide scavengers in oil and gas industry: a review. NAFTA 61 (2), 85–92.

Attia, A.M., 2005. Effects of petrophysical rock properties on tortuosity factor. J. Petrol. Sci. Eng. 48 (3–4), 185–198. https://doi.org/10.1016/j.petrol.2005.06.012.

Bérest, P., Brouard, B., 2003. Safety of salt caverns used for underground storage: blow out, mechanical instability, seepage, cavern abandonment. Oil Gas Sci. Technol. 58 (3), 361–384.

Bernardez, L.A., de Andrade Lima, L.R., de Jesus, E.B., Ramos, C.L.S., Almeida, P.F., 2013. A kinetic study on bacterial sulfate reduction. Bioprocess Biosyst. Eng. 36 (12), 1861–1869. https://doi.org/10.1007/s00449-013-0960-0.

Church, C.D., Wilkin, R.T., Alpers, C.N., Rye, R.O., McCleskey, R.B., 2007. Microbial sulfate reduction and metal attenuation in pH 4 acid mine water. Geochem. Trans. 8 (10) https://doi.org/10.1186/1467-4866-8-10.

Cord-Ruwisch, R., Kleinitz, W., Widdel, F., 1987. Sulfate-reducing bacteria and their activities in oil production. J. Petrol. Technol. 39 (01), 97–106.

Crotogino, F., 2016. Larger scale hydrogen storage. In: Letcher, T.M. (Ed.), Storing Energy with Special Reference to Renewable Energy Sources, first ed. Elsevier, Amsterdam, Oxford, Cambridge, pp. 411–429.

Deutscher Verein des Gas und Wasserfaches, 2013. Technische Regel-Arbeitsblatt DVGW G 260 (A), Gasbeschaffenheit.

Ehrlich, H.L., 1990. Geomicrobiology, second ed. Dekker, New York. 646 pp.

Evans, D.J., 2008. An Appraisal of Underground Gas Storage Technologies and Incidents, for the Development of Risk Assessment Methodology. HSE Books.

Ewing, R.P., Hu, Q., Liu, C., 2010. Scale dependence of intragranular porosity, tortuosity, and diffusivity. Water Resour. Res. 46 (6), 54. https://doi.org/10.1029/2009WR008183.

Fontenot, D.J., 1981. Degassing Method and Apparatus, US4417907 a.

Fu, Y., van Berk, W., Schulz, H.-M., 2016. Hydrogen sulfide formation, fate, and behavior in anhydrite-sealed carbonate gas reservoirs: a three-dimensional reactive mass transport modeling approach. AAPG Bull. 100 (05), 843–865. https://doi.org/10.1306/12111514206.

Ghassemi, A., Pak, A., 2011. Pore scale study of permeability and tortuosity for flow through particulate media using Lattice Boltzmann method. Int. J. Numer. Anal. Meth. Geomech. 35 (8), 886–901. https://doi.org/10.1002/nag.932.

Haddenhorst, H.-G., 1989. Storage of natural gas in salt caverns. In: Tek, M.R. (Ed.), Underground Storage of Natural Gas. Kluwer Academic Publishers, pp. 177–195.

Hsieh, P.A., Winston, R.B., 2002. User's Guide to Model Viewer, a Program for Three-dimensional Visualization of Groundwater Model Results. U.S. Geological Survey Open-File Report, 18 pp.

Jakobsen, R., Postma, D., 1994. In situ rates of sulfate reduction in an aquifer (Rømø, Denmark) and implications for the reactivity of organic matter. Geology 22 (12), 1101. https://doi.org/10.1130/0091-7613(1994)022<1103:ISROSR>2.3.CO;2.

Jorgensen, B.B., Isaksen, M.F., Jannasch, H.W., 1992. Bacterial sulfate reduction above 100 °C in deep-sea hydrothermal vent sediments. Science 258 (5089), 1756–1757. https://doi.org/10.1126/science.258.5089.1756.

Kallmeyer, J., Boetius, A., 2004. Effects of temperature and pressure on sulfate reduction and anaerobic oxidation of methane in hydrothermal sediments of guaymas basin. Appl. Environ. Microbiol. 70 (2), 1231–1233. https://doi.org/10.1128/AEM.70.2.1231-1233.2004.

Kjeldsen, K.U., Loy, A., Jakobsen, T.F., Thomsen, T.R., Wagner, M., Ingvorsen, K., 2007. Diversity of sulfate-reducing bacteria from an extreme hypersaline sediment, Great Salt Lake (Utah). FEMS Microbiol. Ecol. 60 (2), 287–298. https://doi.org/10.1111/j.1574-6941.2007.00288.x.

Kleinitz, W., Böhling, E., 2005. Underground Gas Storage in Porous Media - Operating Experience with Bacteria on Gas Quality. Society of Petroleum Engineers SPE 94248. SPE Europe/EAGE Annual Conference Madrid 13–16 June 2005.

Kyle, J.R., Posey, H.H., 1991. Chapter 5 Halokinesis, cap rock development, and salt dome mineral resources. In: Melvin, J.L. (Ed.), Evaporites, Petroleum and Mineral Resources, vol. 50. Elsevier, Amsterdam, Oxford, New York, Tokyo, pp. 413–474.

Machel, H., 2001. Bacterial and thermochemical sulfate reduction in diagenetic settings — old and new insights. Sediment. Geol. 140 (1–2), 143–175. https://doi.org/10.1016/S0037-0738(00)00176-7.

Meulepas, R.J.W., Stams, A.J.M., Lens, P.N.L., 2010. Biotechnological aspects of sulfate reduction with methane as electron donor. Rev. Environ. Sci. Bio/Tech. 9 (1), 59–78. https://doi.org/10.1007/s11157-010-9193-8.

NLWKN, 2015. Grundwassermessstelle Brauel I Stade. Niedersächsisches Ministerium für Umwelt, Energie und Klimaschutz. www.umweltkarten-niedersachsen.de. (Accessed 5 January 2017).

Panfilov, M., 2016. Underground and pipeline hydrogen storage. In: Gupta, R.B., Basile, A., Veziroğlu, T.N. (Eds.), Compendium of Hydrogen Energy. Volume 2: Hydrogen Storage, Distribution and Infrastructure. Elsevier, Cambridge, Waltham, Kidlington, pp. 91–115.

Parkhurst, D.L., Appelo, C., 2013. Description of Input for PHREEQC Version 3-A Computer Program for Speciation, Batch-reaction, One-dimensional Transport, and Inverse Geochemical Calculations. U.S. Geological Survey Techniques and Methods (6-A43).

Parkhurst, D.L., Charlton, S.R., 2010. PHAST Version 2- a Program for Simulating Groundwater Flow, Solute Transport, and Multicomponent Geochemical Reactions. U.S. Geological Survey Techniques and Methods (6-A35).

Postgate, J.R., 1984. The Sulphate-reducing Bacteria, second ed. University Press, Cambridge. 208 pp.

Reitenbach, V., Ganzer, L., Albrecht, D., Hagemann, B., 2015. Influence of added hydrogen on underground gas storage: a review of key issues. Environ. Earth Sci. 73 (11), 6927–6937. https://doi.org/10.1007/s12665-015-4176-2.

Réveillère, B., Azimi, B., Arnold, C., 2016. Prevention of Stored Gas Humidification: Lessons Learnt and Review of Possibilities. Solution Mining Research Institute Spring, 2016 Technical Conference.

Schneider, R., Crotogino, F., 2010. New developments in Europe's salt cavern projects. In: Hou, M.Z., Xie, H., Yoon, J.S. (Eds.), Underground Storage of CO2 and Energy. CRC Press, Taylor & Francis Group, Boca Raton, Fla, pp. 199–205.

Shen, L., Chen, Z., 2007. Critical review of the impact of tortuosity on diffusion. Chem. Eng. Sci. 62 (14), 3748–3755. https://doi.org/10.1016/j.ces.2007.03.041.

Timmers, P.H., Suarez-Zuluaga, D.A., van Rossem, M., Diender, M., Stams, A.J., Plugge, C.M., 2016. Anaerobic oxidation of methane associated with sulfate

reduction in a natural freshwater gas source. ISME J. 10 (6), 1400–1412. https://doi.org/10.1038/ismej.2015.213.
Tuttle, J.H., Dugan, P.R., Randles, C.I., 1969. Microbial sulfate reduction and its potential utility as an acid mine water pollution abatement procedure. Appl. Microbiol. 17 (2), 297–302.
Wang, T., Yang, C., Yan, X., Daemen, J., 2015. Allowable pillar width for bedded rock salt caverns gas storage. J. Petrol. Sci. Eng. 127, 433–444. https://doi.org/10.1016/j.petrol.2015.01.040.
Yang, C., Jing, W., Daemen, J., Zhang, G., Du, C., 2013. Analysis of major risks associated with hydrocarbon storage caverns in bedded salt rock. Reliab. Eng. Syst. Saf. 113, 94–111. https://doi.org/10.1016/j.ress.2012.12.017.
Zimmermann, G., Jacob, G., Lautenschläger, K.-H., Richter, G., Teschner, J., 1986. Wissensspeicher, seventh ed. Dt. Verl. für Grundstoffindustrie, Leipzig. 71 pp.
ZoBell, C.E., 1958. Ecology of sulfate reducing bacteria. Prod. Mon. 22 (7), 12–29.